PERGAMON

Scripta Materialia 45 (2001) 733–738

Scripta MATERIALIA

www.elsevier.com/locate/scriptamat

Orientation effects during grain subdivision and subsequent annealing in coarse-grained tantalum

H.R.Z. Sandim[a*], J.P. Martins[a], and A.F. Padilha[b]

[a]*Department of Materials Engineering -DEMAR FAENQUIL, Lorena, 12600-000, Brazil*
[b]*Department of Metallurgical and Materials Engineering, USP, São Paulo, 05508-900, Brazil*

Received 29 January 2001; accepted 22 May 2001

Abstract

Noticeable orientation effects were observed in two neighboring grains in tantalum during cold rolling and further annealing. The stored energy varied markedly from grain to grain and, consequently, their response to annealing: grain A recrystallized in full extent while grain B was strongly softened by static recovery. © 2001 Acta Materialia Inc. Published by Elsevier Science Ltd. All rights reserved.

Keywords: Tantalum; Cold working; Microstructure; Recrystallization & recovery; EBSD

Introduction

High purity Ta ingots processed by electron beam melting are typical oligocrystalline materials. During cold rolling, noticeable orientation effects were observed concerning grain subdivision of two adjacent grains. The present work attempts to clarify the evolution of deformation microstructure and the differences in terms of stored energy observed in both grains using electron backscattering diffraction (EBSD). These remarkable differences determine the subsequent changes related to annealing; while the first grain displayed full recrystallization, the second grain was softened by intense recovery.

Experimental procedure

A high-purity coarse-grained tantalum ingot was obtained by means of double electron-beam melting. Interstitial (O < 65, N < 5, wt.-ppm) and metallic (W < 55, Fe < 45, Al < 30 and Si < 50, wt.-ppm) impurity contents are in agreement with ASTM-B-364-92. In the initial state the ingot consisted of columnar grains of 10–15 mm width and lengths of 40 mm outside and up to 150 mm in the center. A thick slab (10 mm

* Corresponding author.
E-mail address: hsandim@demar.faenquil.br (H.R.Z. Sandim).

PII: S1359-6462(01)01087-9

in thickness × 75 mm wide × 300 mm long) was cut out from the center of this ingot and then rolled at room temperature without intermediary annealing to a total reduction in thickness of 70% corresponding to a true strain $\varepsilon = 1.3$. Three consecutive bicrystals were cut out from the rolled plate. The prior grain boundary (GB) (referred to the as-cast condition) was aligned nearly parallel to the rolling direction (RD). These bicrystals are formed by the same grains (A and B) and were investigated in the cold-worked state and after vacuum annealing at 900 and 1200°C for 1 h. Vickers hardness tests were carried out along a centerline using a Buehler Micromet 2004 microindenter with a load of 100 g. Backscattered electron images (BSE) were obtained in a LEO 1450-VP scanning electron microscope operating at 10 kV. The EBSD scans were carried out in an area of about 120×100 μm^2. Microtexture evaluation was determined by means of automatic indexing of Kikuchi patterns after suitable image processing in an OPAL Oxford system interfaced to a JEOL JSM-6400 SEM operating at 20 kV. Pole figures and misorientation (ψ) distributions are based on 12,000 measurements for each mapped region. EBSD sampling points were performed in every 1 μm (corresponding to the map pixel size). Two adjacent areas of each grain in the vicinity of the prior GB were scanned.

Results

The substructure developed after cold rolling was found to be very different in each grain. Fig. 1a shows these two grains in close detail at SEM-BSE. A dashed line marks the position of the prior GB. Grain A developed a fine subgrain structure with an average size of about 4 μm. Furthermore, interspersed lamellae making about 35° with respect to the RD are visible (see arrows in Fig. 1c). In a coarse scale, the deformation microstructure of grain B is less homogeneous than grain A. In Fig. 1a, coarse bands are visible within this grain. Along the GB, a narrow region, About 200 μm wide, is observed in grain B suggesting that slip activity occurred in a distinct manner. Within this large region, a coarse substructure (mosaic structure) is found in grain B as shown in Fig. 1d. Far from the GB region, grain B appears structureless at channeling contrast (SEM) with very low contrast among different regions of substructure.

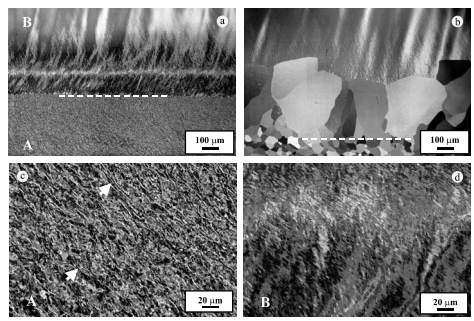

Fig. 1. Microstructure of grains A and B: (a) 70% cold rolled (SEM-BSE); (b) annealed at 1200°C for 1 h; detail of the deformation microstructure close to GB region of grains A (c) and B (d). Dashed line marks the position of the prior GB. (SEM-BSE). RD is parallel to the prior GB shown in (a).

It is worth mentioning that channeling contrast does not resolve all details of the microstructure. This technique allows identifying regions of extension above about 1 μm with misorientations relative to their neighborhood by more than 1°. This does not exclude presence of regions where $\psi > 1°$ provided that the crystallite size within a region is less than 1 μm.

Microhardness testing shows that grain A is much harder than grain B, 134 ± 8 and 97 ± 8 VHN, respectively. After annealing at 1200°C for 1 h, these values dropped to 81 ± 5 and 83 ± 3, respectively. For purposes of comparison, the hardness of as-cast high-purity tantalum is about 66 ± 5 VHN.

The differences in terms of grain subdivision and developed misorientations can be quantified when the microstructure is investigated in detail using EBSD. This technique has a spatial resolution of about 1 μm. Very sharp Kikuchi patterns could be obtained despite of the applied strain. Fig. 2 displays the orientation image mapping (OIM) of both grains at GB region and the corresponding inverse pole figures. Fig. 2a shows that grain A subdivided in a highly misoriented structure. These regions are characterized by displaying a clustered structure resembling bands (green regions). These clusters lie nearly parallel each other making about 35° related to RD. Fig. 2a shows the orientation spread developed within this grain during cold rolling. From data shown in the inverse pole figure, two major orientation components are present: [1 1 4] and near [1 1 0] indicating a large orientation spread in this grain after cold rolling. Contrasting with this feature, grain B appears almost structureless at OIM. According to EBSD results (pole figure), this grain is nearly (0 0 1)[1 1 0]-oriented. Indeed, it is slightly rotated about RD. A few bands are found in this grain corresponding to the orientation scatter displayed in Fig. 2b. They are very diffuse at OIM and can only be distinguished by shading among different regions corresponding to low local lattice misorientations.

The distributions of ψ found in each grain are schematically shown in Fig. 3. Grain A has subdivided in a wide range of misorientations with many boundaries having high angle character ($\psi > 15°$). On the other hand, the cumulative distribution shows that low angle boundaries are predominant in grain B ($\psi < 8°$). The black spots shown in

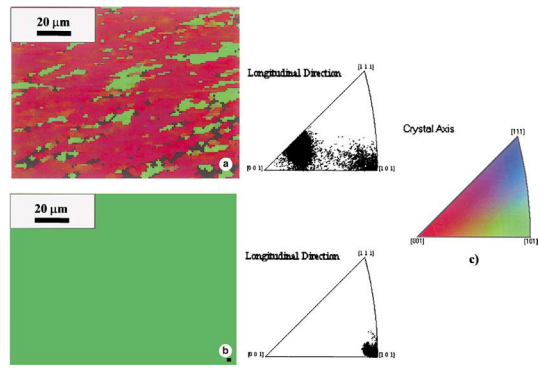

Fig. 2. OIM and inverse pole figures of two adjacent grains of 70% cold-rolled tantalum obtained from 1 μm-spaced EBSD measurements: (a) grain A; (b) grain B; (c) colouring scheme is common for both grains. RD is shown in the left side of each OIM.

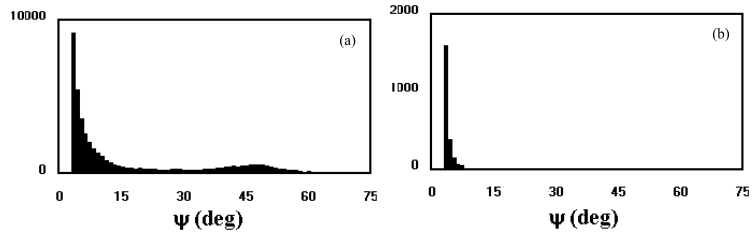

Fig. 3. Histograms showing the distribution of misorientations (Ψ) measured in longitudinal section from EBSD measurements in: (a) grain A and (b) grain B.

both orientation mappings correspond to regions where Kikuchi patterns resulting from the beam-specimen interaction could not be resolved for any reason. In both cases only boundaries with $\psi > 2°$ were taken into account. This has to do with the limited angular accuracy of the OIM-SEM technique.

In consequence of the pronounced differences in the deformation microstructure, these grains did behave quite inhomogeneously during annealing. Strong local differences in the rate of static recrystallization were observed. One advantage of investigating oligocrystals is the possibility of trace individual grains. While grain A displayed full recrystallization when annealed at 1200°C for 1 h, grain B exhibited intense recovery. Annealing at an intermediary temperature revealed the existence of preferential sites for recrystallization in grain A. At 900°C the volume fraction of recrystallized grains was about 50%. The majority of grains were found in the prior GB region. A few isolated grains were also observed in the microstructure. In a quite contrasting way, recrystallization was absent in grain B.

The grain size heterogeneity is evident in grain A. At 1200°C it was observed that recrystallized grains nucleated in grain A grew into grain B. The grain boundaries were driven by the remaining stored energy in grain B giving rise to a wide band consisting of well oriented grains as shown in Fig. 1b. They differ significantly in size and orientation when compared to the majority of the recrystallized grains found in the former grain A. These large elongated grains are about 1 mm in size while the remaining grains are about 100 μm.

Discussion

It is very well known that grains subdivide during plastic deformation [1,2]. The microstructural evolution of tantalum during cold rolling can be described in terms of grain subdivision by generation of geometrically necessary boundaries to accommodate the increasing lattice misorientations [2,3]. Thus, neighboring regions inside a grain with different slip activity are bounded by planar boundaries that take account of the increasing misorientation between those regions. At high strains ($\varepsilon \approx 1$), most of these dislocation boundaries tend to reorient into a lamellar structure having a wide range of misorientations, many of them with high angle character [4,5]. The tendency of grain subdivision into lamellae of strongly different orientations is distinctly orientation-dependent [5]. In a previous paper, the heterogeneity of deformation microstructure in

coarse-grained tantalum deformed by cold swaging was reported [6]. The majority of grains subdivided into a lamellar structure whereas a few grains appeared structureless at SEM or displayed coarse substructured features (e.g. mosaic structure). Another evidence of such dependence is given in Ref. [7]. Different dislocation structures as well as work-hardening behaviors were identified on cold rolling of tantalum single crystals. Depending on their initial orientation, noticeable differences in terms of recrystallization behavior were observed. For instance, $(0\,0\,1)[1\,\bar{1}\,0]$-oriented crystals displayed no recrystallization even after annealing at 1400°C.

The results shown in this investigation confirm that the deformation behavior of each grain depends clearly on their initial orientation. It is well known that nucleation and growth of new grains in a deformed material is driven by the stored energy within each grain. The stored energy depends on the nature and misorientation range of the deformation induced dislocation boundaries. In particular, deformation-induced boundaries with high angle character act as potential nucleation sites for recrystallization. In that sense, the EBSD technique combined to channelling contrast at SEM provides a powerful tool to investigate the deformed state and the early stages of recrystallization.

From the above-presented results, it is clear that grain A has a much higher stored energy compared to grain B. The presence of many boundaries with high angle character (Fig. 3a) explains why grain A recrystallized with ease and grain B did not. In the specimen annealed at 900°C for 1 h, the majority of the recrystallized grains are found predominantly in the vicinity of the prior GB. A few isolated grains with elongated shape are found throughout the deformed matrix. These features confirm that nucleation is far from being a homogeneous process and tends to occur initially at deformation heterogeneities. At 1200°C for 1 h, recrystallization is complete in grain A. An interesting aspect is the presence of elongated grains at the prior GB region in the specimen annealed at 1200°C (Fig. 1b). These grains have probably been nucleated in grain A (or at the GB) and migrated towards grain B driven by its stored energy. This advantage in growth can be explained by the lack of competing grains nucleated in grain B or by orientation effects [8]. It is important to note that equiaxed grains are predominant in the prior GB region in the specimen annealed at 900°C.

The presence of structureless regions in the longitudinal section of grain B means that the deformation must have been quite homogeneous. EBSD has shown that grain B is nearly $(0\,0\,1)[1\,1\,0]$ oriented. In consequence, this grain did not develop potential nuclei for recrystallization. For special orientations with low Taylor factor, e.g. $\{0\,0\,1\}\langle 1\,1\,0\rangle$, deformation occurs in a stable mode resulting in homogeneous deformation and low misorientation of neighboring regions [9,10]. Low-misoriented dislocation structures ($\psi \approx 0.5°$) have also been reported in earlier TEM-investigations of deformed tantalum [11,12]. Results show that recrystallization is suppressed in grain B due to the absence of areas with large local misorientations within the deformation microstructure to provide new boundaries with high-angle character during nucleation [10,13]. It is also possible to argue that this recovered substructure could be swept by migrating grains originally nucleated in grain A if annealing takes place at higher temperatures or longer times. This migration could be driven by the remaining stored energy in the microstructure of grain B. The presence of tiny and elongated unrecrystallized regions in

annealed specimens is commonly observed in tantalum plates obtained by rolling in a direction parallel to the ingot centerline [14,15]. These bands did not disappear even when annealed at higher temperatures and may act as potential defects on further deep drawing of tantalum parts.

The results shown in the present work depict in detail how complex are both deformation and annealing processes in very coarse-grained tantalum. A very similar behavior has been observed in tantalum in a much higher strain, i.e. 90% cold rolled [16].

Conclusions

Noticeable differences in grain subdivision were observed in detail in two adjacent grains of 70% cold rolled tantalum using channelling contrast at SEM combined with orientation mapping provided by EBSD measurements. Grain A subdivided into regions bounded by a wide range of misorientations, many with high angle character. Grain B, on the other hand, deformed in a very stable way giving rise to a low misoriented substructure ($\psi < 8°$). In consequence, the stored energy varied markedly from grain–grain and, consequently, their response to annealing: grain A recrystallized in full extent while grain B was strongly softened by static recovery.

Acknowledgements

The authors are greatly indebted to Prof. Dr. W. Blum and M. Riemer (Universität Erlangen-Nürnberg, Erlangen, Germany) for helpful discussions and their valuable assistance in EBSD measurements and to FAPESP (Brazil) for the financial support. Thanks are also due to Prof. Dr. H.P. Stüwe (Austrian Academy of Sciences, Leoben, Austria) and to Dr. F. Siciliano Jr. (University of Sao Paulo, Brazil) for going through the manuscript meticulously.

References

[1] Hansen, N. (1985). Metall Trans A 16, 2167–2190.
[2] Hansen, N. (1990). Mater Sci Technol 6, 1039–1047.
[3] Bay, B., Hansen, N., & Kuhlmann-Wilsdorf, D. (1992). Mater Sci Eng A 158, 139–146.
[4] Hughes, D. A., & Hansen, N. (1993). Metall Trans A 24, 2021.
[5] Hughes, D. A., & Hansen, N. (1997). Acta Mater 45, 3871.
[6] Sandim, H. R. Z., McQueen, H. J., & Blum, W. (1999). Scripta Mater 42, 151–155.
[7] Vandermeer, R. A., & Snyder Jr., W. B. (1979). Metall Trans A 10, 1031–1044.
[8] Juul Jensen, D. (1992). Scripta Metall Mater 27, 533–538.
[9] Raabe, D., Mülders, B., Gottstein, G., & Lücke, K. (1994). Mater Sci Forum 157–162, 841–846.
[10] Raabe, D., Roters, F., & Marx, V. (1996). Textures Microstruct 26–27, 611–635.
[11] Clark, J. B., Garret Jr., R. K., Jungling, T. L., & Asfahani, R. I. (1991). Metall Trans A 22, 2959–2968.
[12] Murr, L. E., Niou, C. S., Pappu, S., Rivas, J. M., & Quinones, S. A. (1995). Phys Stat Sol (a) 149, 253–274.
[13] Raabe, D. (1995). Steel Res 66, 222–229.
[14] Clark, J. B., Garret Jr., R. K., Jungling, T. L., & Asfahani, R. I. (1991). Metall Trans A 22, 2959–2968.
[15] Clark, J. B., Garret Jr., R. K., Jungling, T. L., & Asfahani, R. I. (1992). Metall Trans A 23, 2183–2191.
[16] H.R.Z. Sandim, unpublished.